Remolding and Deconstruction of Industrial Thermosets via Carboxylic Acid-Catalyzed Bifunctional Silyl Ether Exchange

Keith E. L. Husted, Christopher M. Brown, Peyton Shieh, Ilia Kevlishvili, Samantha L. Kristufek, Hadiqa Zafar, Joseph V. Accardo, Julian C. Cooper, Rebekka S. Klausen, Heather J. Kulik, Jeffrey S. Moore, Nancy R. Sottos, Julia A. Kalow, and Jeremiah A. Johnson

ABSTRACT: Convenient strategies for the deconstruction and reprocessing thermosets could improve the circularity of these materials, but most approaches developed date do not involve to established, high-performance engineering materials. Here, we show that bifunctional silvl ether, i.e., R'O-SiR2-OR", (BSE)based comonomers generate covalent adaptable network analogues of the



industrial thermoset polydicyclopentadiene (pDCPD) through a novel BSE exchange process facilitated by the low-cost food-safe catalyst octanoic acid. Experimental studies and density functional theory calculations suggest an exchange mechanism involving silyl ester intermediates with formation rates that strongly depend on the Si–R2 substituents. As a result, pDCPD thermosets manufactured with BSE comonomers display temperature- and time-dependent stress relaxation as a function of their substituents. Moreover, bulk remolding of pDCPD thermosets is enabled for the first time. Altogether, this work presents a new approach toward the installation of exchangeable bonds into commercial thermosets and establishes acid-catalyzed BSE exchange as a versatile addition to the toolbox of dynamic covalent chemistry.

INTRODUCTION

Thermosets are produced globally on a 65-million-ton per year scale, accounting for nearly 20% of all polymer production by mass. (1) These materials are often difficult to recycle or upcycle and are generally incinerated or sent to landfills at the end of their usage lifetime, posing mounting environmental hazards. (2–8) Thermosets with dynamically exchangeable covalent bonds, referred to as "covalent adaptable networks" (CANs), could offer new end-of-life options for this class of materials by enabling reprocessing (through bond exchange) or triggered deconstruction (through bond cleavage) to generate functional products for recycling and upcycling; (2,9–28) however, strategies for the incorporation of dynamic covalent bonds into industrially relevant, permanently crosslinked thermosets are lacking. Most CANs reported to date are either (1) thermosets with intrinsically exchangeable bonds (e.g., certain polyurethanes and polyesters); (29,30) (2) thermoplastics crosslinked with dynamic crosslinkers to form new CANs; (9) or (3) new materials derived from bespoke components. (2,14,16,28,31–34) Although promising, these strategies do not enable facile manufacturing of CANs based on commercial, permanently crosslinked thermosets.

Polydicyclopentadiene (pDCPD) is a high-performance industrial thermoset with good chemical and thermal stability, a high glass transition temperature (Tg, ca. 155–175 °C), excellent ballistic impact resistance, (35–37) versatile manufacturing pathways, (38) and tunable properties. (39–42) Moreover, it has considerable industrial relevance with a market value estimated to be >\$700 M USD per year. (43) Here, we introduce a new approach to CAN synthesis that involves the installation of dynamic covalent bonds directly into the strands of a pDCPD thermoset network. The synthetic modification is minor, requiring only a comonomer containing a bifunctional silyl ether (BSE), i.e., R'O–SiR2–OR" (Scheme 1a), the incorporation of which does not affect the

tensile properties or impact resistance of pDCPD at loadings up to 10% v/v. (44) We demonstrate a novel method for dynamic covalent bond exchange that is based on the acid-catalyzed cleavage and reformation of BSEs using the low-cost food additive octanoic acid (OA), offering a versatile strategy to either deconstruct or achieve macroscopic remolding of pDCPD. Mechanistic experiments and density functional theory (DFT) calculations suggest that BSE exchange occurs through an OA-based silyl ester intermediate and that the rate of exchange is tuned through simple variations of the BSE silicon substituents. Altogether, this work introduces dynamic covalent chemistry using BSEs and a comonomer approach for converting permanently crosslinked industrial thermosets into CANs.

SCHEME 1

a) Synthesis of bifunctional silyl ether (BSE)-based monomers

b) Previous work: Deconstruction of BSE-containing thermosets via bond cleavage

c) This work: Network rearrangement in BSE-containing thermosets via bond exchange

Scheme 1. (a-c) Preparation of BSEs and BSE-Containing pDCPD Materials

RESULTS AND DISCUSSION

Discovery of Octanoic Acid-Catalyzed BSE Exchange

We previously showed that BSE-containing 7- or 8-membered cyclic olefins (Scheme 1a) copolymerize with DCPD to produce chemically deconstructable pDCPD thermosets (Scheme 1b). At sufficient comonomer loadings to overcome the permanent crosslink density of pDCPD (~7% v/v), these modified thermosets are solubilized by treatment with fluoride or 1 M HCl to generate pDCPD fragments for recycling or upcycling schemes (Scheme 1b). (44–46)

Here, we hypothesized that BSEs can undergo exchange reactions rather than cleavage; if validated, thermosets manufactured using BSE-containing comonomers could behave as CANs under suitable conditions, allowing stress relaxation, healing, or remolding, while maintaining their capability for orthogonal deconstruction (Scheme 1c). This hypothesis is inspired by reports of Si–O bond exchange in related Si-containing functional groups and polymeric systems. For example, as early as 1954, it was known that strong acids or bases could catalyze Si–O exchange in siloxanes (Si–O–Si groups) such as polydimethylsiloxane (PDMS) (Figure 1a). (47–49) Later, Guan and co-workers reported alcohol-induced Si–O bond exchange in trialkoxysilane crosslinked materials (Figure 1b) (11) as well as a proposed direct Si–O bond metathesis in mono-

silyl ether-crosslinked materials (Figure 1c). (10,11) Additionally, Du Prez and co-workers proposed an associative silanol-induced siloxane exchange process to achieve similar material remodeling (Figure 1d). (50) While these studies provide strong precedent for Si–O bond exchange in crosslinked materials, we note that there are no reports on Si–O bond exchange in BSEs (Figure 1e) despite their use as cleavable functionalities in polymers and related systems. (44–46,51–58) Moreover, BSEs could offer greater control over the rate of network reconfiguration than other Si-based systems. We posit that the Si substituents in BSE-based materials—which are known to dramatically influence the rate of Si–O bond cleavage and of which hundreds of variants are readily synthesized from commercially available precursors (52,53,59)—will provide a route to control CAN stress relaxation dynamics. Finally, each of the previously reported approaches utilizes either inherently exchangeable bonds in elastomers (PDMS) or bespoke CANs; they have not been introduced into industrially relevant thermoset plastics that possess permanent crosslinks.

To test our hypotheses, we first explored conditions for catalytic BSE exchange using acyclic model compounds 1-R and 2-R (Figure 2a), where R refers to the Si alkyl substituents iPr, Et, or Me (Figures S1–S12). Exposure of a 1:1 molar ratio of 1-iPr and 2-iPr to various potential catalysts (Figure S13) for 18 h at 180 °C gave hints of successful bond exchange as determined by observation of the crossover product 3-iPr by gas chromatography-mass spectrometry (GC-MS) (see the Supporting Information for full experimental details). While a negligible amount of 3-iPr was observed in the absence of a catalyst, OA, camphorsulfonic acid (CSA), and 1,8diazabicyclo[5.4.0]undec-7-ene (DBU), all yielded substantial amounts of 3-iPr as estimated from relative peak intensities. By contrast, NH4Cl and Zn(acac)2 gave little crossover product. Based on these results, we chose to move forward with OA for several reasons: (1) it is soluble in the DCPD monomer at all loadings tested; (2) it is compatible with DCPD curing and pDCPD thermosets (treatment of pDCPD with CSA led to severe discoloration, Figure S14); (3) it is readily absorbed into cured pDCPD resins for post-curing addition if desired; (4) it has a high boiling point (237 °C), which will prevent evaporation during oven curing; (5) it is cheap and readily available; and (6) it is safe (OA is found in coconut and palm oils as well as the milk of some mammals, (60) and it has been used as a dietary supplement). (61)

FIGURE 1

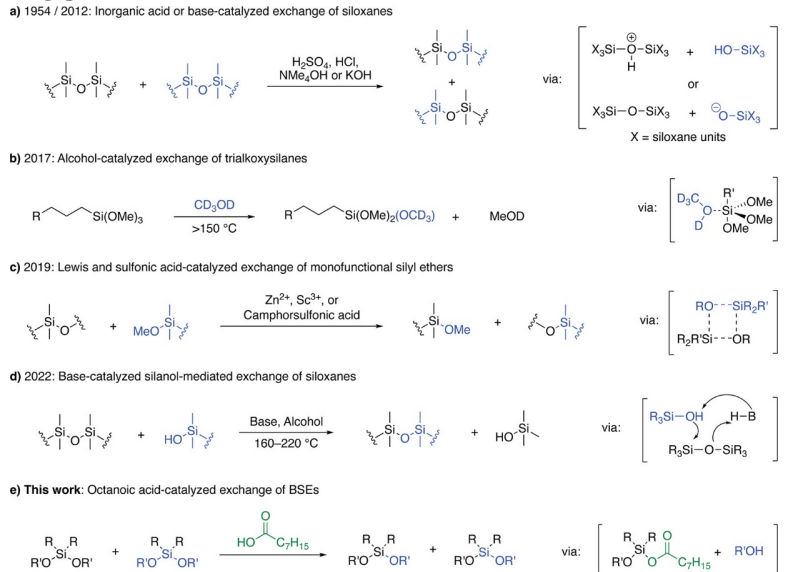


Figure 1. (a-e) Summary of exchange reactions at silicon used for network rearrangement.

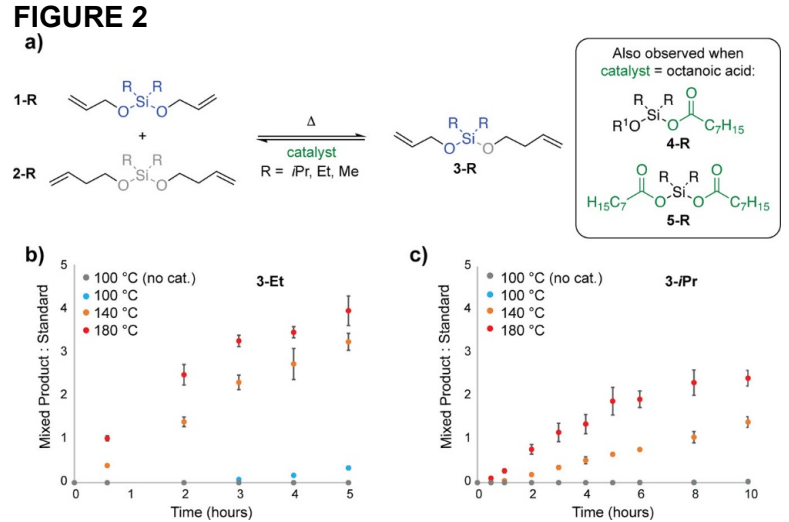


Figure 2. (a) Structures and exchange reactions of allyl and butenyl BSEs of varying silicon substitution R1 = allyl or butenyl. (b) and (c) Analysis of the rate of formation of mixed species 3-R in the early stages (<25% conversion) of the BSE exchange reaction as a function of temperature, catalyst loading, and silicon substitution.

To explore the impacts of temperature and BSE Si substituents on this dynamic covalent bond exchange reaction, analogous crossover experiments were conducted using Me, Et, and iPr derivatives of 1-R and 2-R at temperatures ranging from 60 to 180 °C (Figure 2b,c) (Figures S15–S17). The Si substituents had a major effect on the temperature at which crossover occurs: in the presence of OA catalyst, crossover product 3-R was observed at ~60, 100, and 140 °C, for Me, Et, and iPr, respectively. In the absence of OA, 3-R was observed at 100 and 160 °C for Me and Et, respectively, and was not observed in appreciable amounts for iPr. We note that reactions of 1-Me and 2-Me yielded several side products, including linear and cyclic dimethylsiloxanes, in addition to 3-Me; thus, we focused our subsequent studies on the iPr- and Et-substituted derivatives (Figure S18).

FIGURE 3

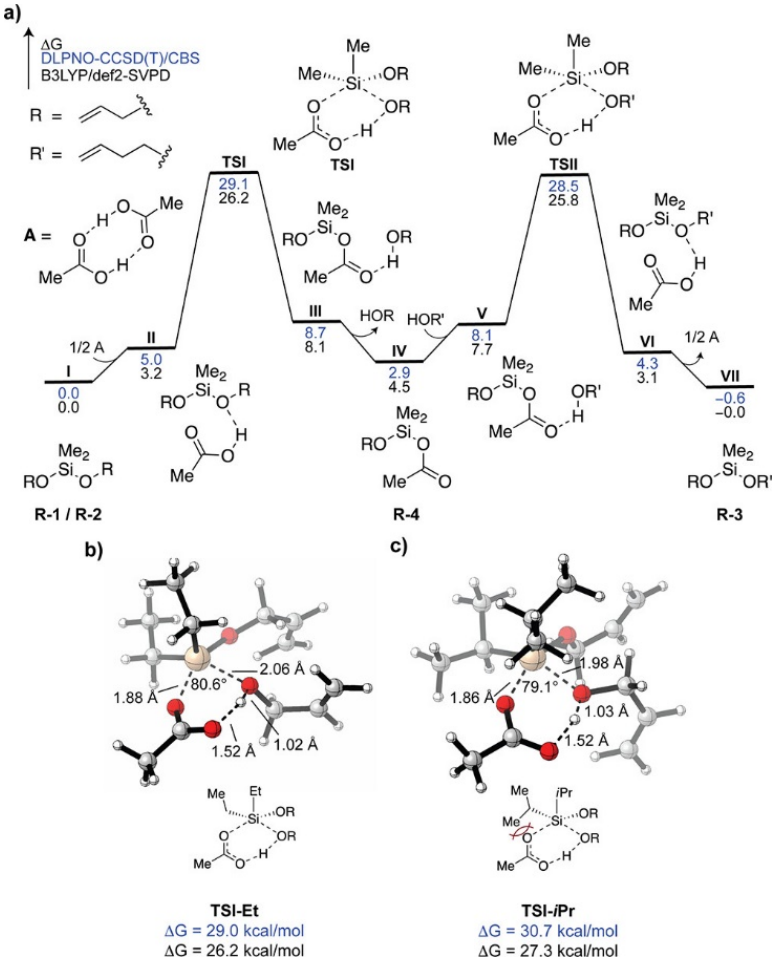


Figure 3. (a) Energy diagram for BSE exchange reaction calculated by DFT (B3LYP/DEF2-SVPD); (b and c) DLPNO-CCSD(T) snapshots of transition states and energies with (b) ethyl and (c) isopropyl Si substituents.

As expected, 3-Et and 3-iPr form faster at higher temperatures, and 3-iPr forms more slowly than 3-Et at all temperatures due presumably to the increased steric hindrance imposed by its iPr substituents (53) (Figures 3a–c, S19 and S20) (see the Supplementary Information for further details). These results support our hypothesis that Si-substituents tune the rate of BSE exchange, which may offer an additional route to manipulating stress relaxation rates in CANs. Mechanistic Studies of BSE Exchange.

Mono- and bis-silyl ester intermediates of the general structure 4-R and 5-R were observed by GC-MS in the OA-catalyzed crossover reactions (Figure S21). Moreover, heating 1-Et in 1.1 equiv of OA (Figure 2a) (Figure S22) led to the slow generation of free allyl alcohol. These results suggest a mechanism involving Si-O bond cleavage prior to exchange analogous to related siloxane exchange reactions (Figure 1a). (62) DFT geometry optimizations (B3LYP/DEF2-SVPD) were carried out to investigate the free energy profile for the transformation of 1-Me and 2-Me to 3-Me using acetic acid as a simplified OA analogue (Figure 3a, reported energies are from DLPNO-CCSD(T) single-point calculations). Cleavage of the BSE through the formation of silyl ester 4-Me and expulsion of allyl alcohol was observed to be slightly endergonic (IV, +2.9 kcal/mol) compared to the acetic acid dimer and BSE (I) and thermally accessible via a six-membered transition state (TSI, +29.1 kcal/mol) involving square pyramidal Si and the catalyst.

Attack of 4-Me by 3-buten-1-ol yields the crossover product 3-Me (VII) through an analogous transition state (TSII).

Electronic structure calculations provided further insight into the Si-substituent effects observed experimentally. First, there was no difference in the calculated energy barriers for the formation of silyl esters 4-Me and 4-Et, which suggests that the faster rate of formation of 3-Me relative to 3-Et experimentally may be due to a greater extent of background reaction in the former case. Nevertheless, bulkier isopropyl substituents caused a +1.7 kcal/mol larger energy barrier for formation of 4-iPr relative to 4-Et, which translates to a ~7–8-fold rate difference at 140 °C (in good agreement with the experimentally observed slower reaction for 1-iPr compared to 1-Et). The origin of this difference is a steric clash between the catalyst and one of the iPr groups of 1-iPr or 2-iPr in the transition state, which is avoided with Me and Et groups (Figure 3b,c). Installing BSEs into Industrial Hydrocarbon Thermosets To Generate Orthogonally Deconstructable and Remoldable CANs.

Having shown that BSEs can undergo Si–O bond cleavage and exchange catalyzed by OA, we next sought to leverage this reaction for the fabrication of pDCPD CANs (Scheme 1c). Cleavable BSE-based comonomers iPrSi7, EtSi7, and MeSi7 were prepared in one step from cis-butene diol and the corresponding dichlorodialkylsilanes (Scheme 1a; Figures S23–S28). pDCPD thermosets were prepared by blending 10% v/v of each BSE comonomer with DCPD and the Grubbs 2nd-generation catalyst (~0.03 mol %) and heating the resulting mixture to 120 °C for 0.5 h in an oven under an ambient atmosphere (Scheme 1b). Treatment of the resulting thermosets with 0.2 M tetrabutylammonium fluoride (TBAF) in tetrahydrofuran overnight led to their dissolution to form alcohol-terminated network fragments (Figure S29), which confirms that BSEs were incorporated into the polymer network strands and that the density of cleavable strands is greater than the effective crosslink density at this BSE loading. (44)

We reasoned that heating these pDCPD thermosets in the presence of excess OA and solvent should induce network deconstruction. Indeed, heating EtSi7 (10% v/v)-containing pDCPD samples in toluene at 110 °C in the presence of OA resulted in material dissolution in an OA dose-dependent fashion. Specifically, near-complete deconstruction was achieved with 2 equiv of OA relative to BSE (Figures S30 and S31), while no deconstruction was observed in the absence of OA or at lower temperatures. This method offers an alternative approach, compared to previously reported TBAF and HCl, to the chemical deconstruction of pDCPD thermosets using a food-safe reagent.

Next, we sought to demonstrate CAN behavior of EtSi7- and iPrSi7-(10% v/v) containing pDCPD thermosets. Rectangular bars (ca. 12 × 3 × 2 mm3) (Figure S32) of six different test and control specimens were prepared for dynamic mechanical analysis (DMA) stress relaxation studies. (44,46) First, test samples iPr+ and Et+ were prepared by curing DCPD in the presence of 10% v/v iPrSi7 or EtSi7 and 1 wt % OA. Control samples that lacked OA catalysts, iPr– and Et–, were prepared following the same procedure but without OA. Additionally, non-BSE control samples were manufactured using cyclooctene (COE, 14% v/v) as a comonomer (41) rather than iPrSi7 or EtSi7 and with (COE+) or without OA (COE–).

We note that the glass transition temperatures (Tg), as estimated by the global maximum in tan (δ) from DMA temperature sweeps (Table S1; Figures S33–S35), of samples prepared in the presence of OA, including the COE control, were 28–37 °C lower than those of materials made in the absence of OA. This observation suggests that OA acts as a plasticizer in these thermosets. Nevertheless, the Tg values across samples with OA and without OA were sufficiently similar

(Table 1) to allow for comparisons of stress relaxation behavior as a function of temperature, BSE substituents, and the presence of OA.

Table 1. Glass Transition Temperatures (Tg) of Comonomer-Containing pDCPD Samples Prepared with (+) and without (-) OA, as Estimated from the Maximum in $tan(\delta)$ of Dynamic Mechanical Analysis Temperature Sweeps

sample	<i>T</i> _g (°C)
EtSi7-	107 ± 1
EtSi7+	90 ± 0.4
iPrSi7-	123 ± 2
iPrSi7+	95 ± 4
COE-	106 ± 2
COE+	79 ± 3

Stress relaxation times were determined as the time required for a sample held at a fixed strain and fixed temperature to relax to 1/e of its initial stress. Stress relaxation was observed in BSE-containing samples that lacked OA, which we attribute to residual olefin metathesis activity as confirmed through the observation of similar incomplete relaxation in COE-based samples (Figure S38). (63) Importantly, the stress relaxation rate was accelerated in samples containing BSEs and OA. For example, EtSi7+ displayed relaxation times of ~100–1000 s over the temperature range of 130–190 °C, which was ~10-fold faster than EtSi7– (Figure 4a). As expected, the stress relaxation rate correlated with Si substituents in these systems: iPrSi7-based samples with OA relaxed stress ~2–3-fold more slowly than their EtSi7 counterparts in the temperature range studied here (Figure 4b). (53) Plots of relaxation time vs 1/T revealed approximately Arrhenius relaxation behavior for both materials (Figure 4c) (Figures S37 and S38), providing estimated activation energies for stress relaxation of 49 and 30 kJ mol–1 for iPrSi7+ and EtSi7+, respectively. While these values do not quantitatively agree with the barriers calculated using DFT due to fundamental differences between polymer network relaxation and vacuum calculations, respectively, (64) the trends that describe the effects of iPr- and Et-substituted BSEs agree well.

FIGURE 4

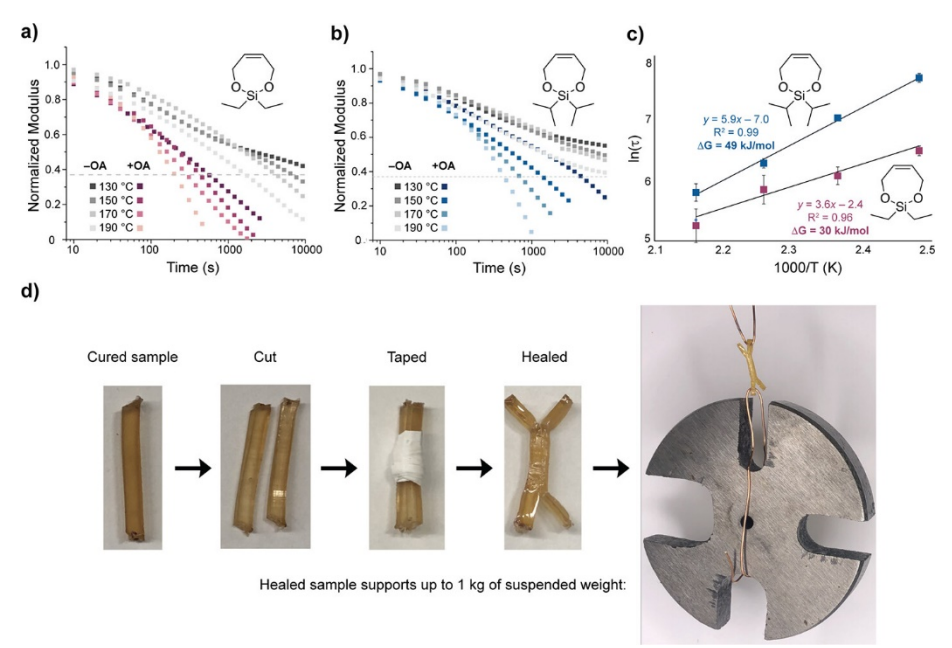


Figure 4. (a, b) DMA stress-relaxation of (a) EtSi7+ and (b) iPrSi7+ pDCPD thermosets cured with (red or blue, respectively) and without (gray) OA. Dashed lines represent normalized moduli of 1/e. (c) Arrhenius plots of stress relaxation for these samples, highlighting the role of Si substituents. (d) Direct remolding of EtSi7+ samples under applied force and temperature yields robust, healed materials.

Macroscopic remolding or self-healing of damaged materials under an applied stimulus is another common way to demonstrate CAN behavior. Initially, we found that damaged pDCPD samples containing BSEs could not be remolded into cohesive materials. We hypothesized that healing was prevented by oxidative crosslinking at the pDCPD surface, (65,66) which would inhibit merging of two separate materials. Indeed, dissolution experiments, X-ray photoelectron spectroscopy, multi-depth nanoindentation, contact angle measurements with and without surface etching, Fourier transform infrared spectroscopy, and small-angle X-ray scattering collectively provided strong evidence for the presence of an oxidized, more crosslinked surface layer of <1000 nm in thickness on these pDCPD samples (see the Supporting Information for a detailed analysis, including Figures S39–S45).

To overcome this challenge, we prepared a new set of EtSi7+ samples with a higher BSE loading (20% v/v) (to further facilitate BSE exchange) and in the presence of the antioxidant butylated hydroxytoluene (BHT, 1 part per hundred, phr, ca. 1 wt %) (to inhibit oxidative crosslinking). Rectangular bars of ~12 × 3 × 2 mm3 were prepared, cut in half lengthwise with a razor blade, immediately wrapped at the centers in Teflon tape with their freshly cut faces pressed together, and placed in a 120 °C oven for 1 h (Figures 4d, S46). After cooling, a 1 kg weight was applied to determine if the two pieces would break apart. Notably, only the sample containing OA (2 phr) and BHT could bear weight; samples lacking either OA or BHT immediately delaminated. Thus, while the risk of oxidative crosslinking inherent to unsaturated polyolefins (such as pDCPD) presents a challenge to the practical reprocessing of these materials, our results suggest that OA-catalyzed BSE exchange can enable macroscopic pDCPD healing. In the future, surface coatings/modifications may also offer routes to address this challenge.

CONCLUSIONS

This work introduces a new way to install exchangeable bonds into an industrial thermoset using comonomers containing BSEs. Moreover, OA, a safe and widely available reagent, was shown to catalyze BSE exchange, enabling either thermoset deconstruction or macroscopic remolding. The rate of BSE exchange is strongly dependent on the silicon substituents of the BSE, providing a range of tunability. This work adds a new reaction to the toolbox of dynamic covalent chemistry and establishes a strategy for the introduction of exchangeable bonds into permanently crosslinked networks using comonomers. Finally, we propose that this strategy of incorporating exchangeable bonds into thermoset strands via copolymerization with cleavable/exchangeable comonomers could be applied to any thermoset material, so long as a suitable comonomer can be identified.

ACKNOWLEDGEMENTS

This work was supported by the NSF Center for the Chemistry of Molecularly Optimized Networks (MONET), CHE-2116298. K.E.L.H. acknowledges support from the National Sciences and Engineering Research Council of Canada (for the NSERC PGSD fellowship). C.M.B. acknowledges NSERC for a Postdoctoral Fellowship. H.Z. acknowledges the National Science Foundation Graduate Research Fellowship Grant no. 2141064 for funding. This work used Expanse at San Diego Supercomputing Center through allocation CHE140073 from the Advanced Cyberinfrastructure Coordination Ecosystem: Services and Support (ACCESS) program, which is supported by National Science Foundation Grants #2138259, #2138286, #2138307, #2137603, and #2138296.

REFERENCES

- 1) Geyer, R.; Jambeck, J. R.; Law, K. L. Production, Use, and Fate of All Plastics Ever Made. *Sci. Adv.* 2017, 3, e1700782 DOI: 10.1126/sciadv.1700782
- 2) Fortman, D. J.; Brutman, J. P.; De Hoe, X. G.; Snyder, L. R.; Dichtel, R. W.; Hillmyer, A. M. Approaches to Sustainable and Continually Recyclable Cross-Linked Polymers. *ACS Sustainable Chem. Eng.* 2018, 6, 11145–11159, DOI: 10.1021/acssuschemeng.8b02355
- 3) Schneiderman, D. K.; Hillmyer, M. A. 50th Anniversary Perspective: There Is a Great Future in Sustainable Polymers. *Macromolecules* 2017, 50, 3733–3749, DOI: 10.1021/acs.macromol.7b00293
- 4) Post, W.; Susa, A.; Blaauw, R.; Molenveld, K.; Knoop, R. J. I. A Review on the Potential and Limitations of Recyclable Thermosets for Structural Applications. *Polym. Rev.* 2020, 60, 359–388. DOI: 10.1080/15583724.2019.1673406
- 5) Long, T. E. Toward Recyclable Thermosets. *Science* 2014, 344, 706–707, DOI: 10.1126/science.1254401
- 6) Billiet, S.; Trenor, S. R. 100th Anniversary of Macromolecular Science Viewpoint: Needs for Plastics Packaging Circularity. *ACS Macro Lett.* 2020, 9, 1376–1390, DOI: 10.1021/acsmacrolett.0c00437
- 7) Klemeš, J. J.; Fan, Y. V.; Jiang, P. Plastics: Friends or Foes? The Circularity and Plastic Waste Footprint. Energy Sources A Recovery *Util. Environ. Eff.* 2020, 43, 1549–1565, DOI: 10.1080/15567036.2020.1801906

- 8) Bakshi, B. R.; Shonnard, D.; Allen, D. T. *ACS Sustainable Chem. Eng.* 2021, 9, 1425–1426, DOI: 10.1021/acssuschemeng.1c00209
- 9) Röttger, M.; Domenech, T.; Van Der Weegen, R.; Breuillac, A.; Nicolaÿ, R.; Leibler, L. High-Performance Vitrimers from Commodity Thermoplastics through Dioxaborolane Metathesis. *Science* 2017, 356, 62–65, DOI: 10.1126/science.aah5281
- 10) Tretbar, C. A.; Neal, J. A.; Guan, Z. Direct Silyl Ether Metathesis for Vitrimers with Exceptional Thermal Stability. *J. Am. Chem. Soc.* 2019, 141, 16595– 16599, DOI: 10.1021/jacs.9b08876
- 11) Nishimura, Y.; Chung, J.; Muradyan, H.; Guan, Z. Silyl Ether as a Robust and Thermally Stable Dynamic Covalent Motif for Malleable Polymer Design. *J. Am. Chem. Soc.* 2017, 139, 14881–14884, DOI: 10.1021/jacs.7b08826
- 12) Houck, H. A.; Blasco, E.; Du Prez, F. E.; Barner-Kowollik, C. Light-Stabilized Dynamic Materials. *J. Am. Chem. Soc.* 2019, 141, 12329–12337, DOI: 10.1021/jacs.9b05092
- 13) Zou, W.; Dong, J.; Luo, Y.; Zhao, Q.; Xie, T. Dynamic Covalent Polymer Networks: From Old Chemistry to Modern Day Innovations. *Adv. Mater.* 2017, 29, 1606100 DOI: 10.1002/adma.201606100
- 14) Lessard, J. J.; Scheutz, G. M.; Hyun Sung, S.; Lantz, K. A.; Epps, T. H.; Sumerlin, B. S. Block Copolymer Vitrimers. *J. Am. Chem. Soc.* 2020, 142, 283–289, DOI: 10.1021/jacs.9b10360
- 15) Kloxin, C. J.; Bowman, C. N. Covalent Adaptable Networks: Smart, Reconfigurable and Responsive Network Systems. *Chem. Soc. Rev.* 2013, 42, 7161–7173, DOI: 10.1039/C3CS60046G
- 16) Winne, J. M.; Leibler, L.; Du Prez, F. E. Dynamic Covalent Chemistry in Polymer Networks: A Mechanistic Perspective. *Polym. Chem.* 2019, 10, 6091–6108, DOI: 10.1039/C9PY01260E
- 17) Christensen, P. R.; Scheuermann, A. M.; Loeffler, K. E.; Helms, B. A. Closed-Loop Recycling of Plastics Enabled by Dynamic Covalent Diketoenamine Bonds. *Nat. Chem.* 2019, 11, 442–448, DOI: 10.1038/s41557-019-0249-2
- 18) Mo, R.; Song, L.; Hu, J.; Sheng, X.; Zhang, X. An Acid-Degradable Biobased Epoxy-Imine Adaptable Network Polymer for the Fabrication of Responsive Structural Color Film. *Polym. Chem.* 2020, 11, 974–981, DOI: 10.1039/C9PY01821B
- 19) Xu, X.; Ma, S.; Wang, S.; Wu, J.; Li, Q.; Lu, N.; Liu, Y.; Yang, J.; Feng, J.; Zhu, J. Dihydrazone-Based Dynamic Covalent Epoxy Networks with High Creep Resistance, Controlled Degradability, and Intrinsic Antibacterial Properties from Bioresources. *J. Mater. Chem. A* 2020, 8, 11261–11274, DOI: 10.1039/D0TA01419B
- 20) Breuillac, A.; Kassalias, A.; Nicolaÿ, R. Polybutadiene Vitrimers Based on Dioxaborolane Chemistry and Dual Networks with Static and Dynamic Cross-Links. *Macromolecules* 2019, 52, 7102–7113, DOI: 10.1021/acs.macromol.9b01288

- 21) Li, Q.; Ma, S.; Li, P.; Wang, B.; Feng, H.; Lu, N.; Wang, S.; Liu, Y.; Xu, X.; Zhu, J. Biosourced Acetal and Diels–Alder Adduct Concurrent Polyurethane Covalent Adaptable Network. *Macromolecules* 2021, 54, 1742–1753, DOI: 10.1021/acs.macromol.0c02699
- 22) Denissen, W.; Rivero, G.; Nicolaÿ, R.; Leibler, L.; Winne, J. M.; Du Prez, F. E. Vinylogous Urethane Vitrimers. *Adv. Funct. Mater.* 2015, 25, 2451–2457, DOI: 10.1002/adfm.201404553
- 23) Obadia, M. M.; Mudraboyina, B. P.; Serghei, A.; Montarnal, D.; Drockenmuller, E. Reprocessing and Recycling of Highly Cross-Linked Ion-Conducting Networks through Transalkylation Exchanges of C–N Bonds. *J. Am. Chem. Soc.* 2015, 137, 6078–6083, DOI: 10.1021/jacs.5b02653
- 24) Jourdain, A.; Asbai, R.; Anaya, O.; Chehimi, M. M.; Drockenmuller, E.; Montarnal, D. Rheological Properties of Covalent Adaptable Networks with 1,2,3-Triazolium Cross-Links: The Missing Link between Vitrimers and Dissociative Networks. *Macromolecules* 2020, 53, 1884–1900, DOI: 10.1021/acs.macromol.9b02204
- 25) Fang, H.; Ye, W.; Ding, Y.; Henning Winter, H. Rheology of the Critical Transition State of an Epoxy Vitrimer. *Macromolecules* 2020, 53, 4855–4862, DOI: 10.1021/acs.macromol.0c00843
- 26) Delahaye, M.; Winne, J. M.; Du Prez, F. E. Internal Catalysis in Covalent Adaptable Networks: Phthalate Monoester Transesterification As a Versatile Dynamic Cross-Linking Chemistry. *J. Am. Chem. Soc.* 2019, 141, 15277–15287, DOI: 10.1021/jacs.9b07269
- 27) Hajj, R.; Duval, A.; Dhers, S.; Avérous, L. Network Design to Control Polyimine Vitrimer Properties: Physical Versus Chemical Approach. *Macromolecules* 2020, 53, 3796–3805, DOI: 10.1021/acs.macromol.0c00453
- 28) Wang, S.; Ma, S.; Li, Q.; Xu, X.; Wang, B.; Huang, K.; Liu, Y.; Zhu, J. Facile Preparation of Polyimine Vitrimers with Enhanced Creep Resistance and Thermal and Mechanical Properties via Metal Coordination. *Macromolecules* 2020, 53, 2919–2931, DOI: 10.1021/acs.macromol.0c00036
- 29) Brutman, J. P.; Fortman, D. J.; De Hoe, G. X.; Dichtel, W. R.; Hillmyer, M. A. Mechanistic Study of Stress Relaxation in Urethane-Containing Polymer Networks. *J. Phys. Chem. B* 2019, 123, 1432–1441, DOI: 10.1021/acs.jpcb.8b11489
- 30) Shi, J.; Zheng, T.; Zhang, Y.; Guo, B.; Xu, J. Reprocessable Cross-Linked Polyurethane with Dynamic and Tunable Phenol–Carbamate Network. *ACS Sustainable Chem. Eng.* 2020, 8, 1207–1218, DOI: 10.1021/acssuschemeng.9b06435
- 31) Li, L.; Chen, X.; Jin, K.; Torkelson, J. M. Vitrimers Designed Both To Strongly Suppress Creep and To Recover Original Cross-Link Density after Reprocessing: Quantitative Theory and Experiments. Macromolecules 2018, 51, 5537–5546, DOI: 10.1021/acs.macromol.8b00922
- 32) Li, L.; Chen, X.; Torkelson, J. M. Reprocessable Polymer Networks via Thiourethane Dynamic Chemistry: Recovery of Cross-Link Density after Recycling and Proof-of-Principle Solvolysis Leading to Monomer Recovery. *Macromolecules* 2019, 52, 8207–8216, DOI: 10.1021/acs.macromol.9b01359

- 33) Guerre, M.; Taplan, C.; Nicolaÿ, R.; Winne, J. M.; Du Prez, F. E. Fluorinated Vitrimer Elastomers with a Dual Temperature Response. *J. Am. Chem. Soc.* 2018, 140, 13272–13284, DOI: 10.1021/jacs.8b07094
- 34) Mangialetto, J.; Cuvellier, A.; Verhelle, R.; Brancart, J.; Rahier, H.; Van Assche, G.; Van den Brande, N.; Van Mele, B. Diffusion- and Mobility-Controlled Self-Healing Polymer Networks with Dynamic Covalent Bonding. *Macromolecules* 2019, 52, 8440–8452, DOI: 10.1021/acs.macromol.9b01453
- 35) Wang, Y.; Zhang, L.; Sun, J.; Bao, J.-B.; Wang, Z.; Ni, L. Dramatic Toughness Enhancement of Polydicyclopentadiene Composites by Incorporating Low Amounts of Vinyl-Functionalized SiO2. *Ind. Eng. Chem. Res.* 2017, 56, 4750–4757, DOI: 10.1021/acs.iecr.7b00093
- 36) Cuthbert, T. J.; Li, T.; Wulff, J. E. Production and Dynamic Mechanical Analysis of Macro-Scale Functionalized Polydicyclopentadiene Objects Facilitated by Rational Synthesis and Reaction Injection Molding. *ACS Appl. Polym. Mater.* 2019, 1, 2460–2471, DOI: 10.1021/acsapm.9b00571
- 37) Le Gac, P. Y.; Choqueuse, D.; Paris, M.; Recher, G.; Zimmer, C.; Melot, D. Durability of Polydicyclopentadiene under High Temperature, High Pressure and Seawater (Offshore Oil Production Conditions). *Polym. Degrad. Stab.* 2013, 98, 809–817, DOI: 10.1016/j.polymdegradstab.2012.12.023
- 38) Robertson, I. D.; Pruitt, E. L.; Moore, J. S. Frontal Ring-Opening Metathesis Polymerization of Exo-Dicyclopentadiene for Low Catalyst Loadings. *ACS Macro Lett.* 2016, 5, 593–596, DOI: 10.1021/acsmacrolett.6b00227
- 39) Li, T.; Shumka, H.; Cuthbert, T. J.; Liu, C.; Wulff, J. E. Harnessing the Surface Chemistry of Methyl Ester Functionalized Polydicyclopentadiene and Exploring Surface Bioactivity. *Mater. Adv.* 2020, 1, 1753–1762, DOI: 10.1039/D0MA00480D
- 40) Chen, J.; Burns, F. P.; Moffitt, M. G.; Wulff, J. E. Thermally Crosslinked Functionalized Polydicyclopentadiene with a High Tg and Tunable Surface Energy. *ACS Omega* 2016, 1, 532–540, DOI: 10.1021/acsomega.6b00193
- 41) Dean, L. M.; Wu, Q.; Alshangiti, O.; Moore, J. S.; Sottos, N. R. Rapid Synthesis of Elastomers and Thermosets with Tunable Thermomechanical Properties. *ACS Macro Lett.* 2020, 9, 819–824, DOI: 10.1021/acsmacrolett.0c00233
- 42) Ivanoff, D. G.; Sung, J.; Butikofer, S. M.; Moore, J. S.; Sottos, N. R. Cross-Linking Agents for Enhanced Performance of Thermosets Prepared via Frontal Ring-Opening Metathesis Polymerization. *Macromolecules* 2020, 53, 8360–8366, DOI: 10.1021/acs.macromol.0c01530
- 43) Kim, H. G.; Son, H. J.; Lee, D. K.; Kim, D. W.; Park, H. J.; Cho, D. H. Optimization and Analysis of Reaction Injection Molding of Polydicyclopentadiene Using Response Surface Methodology. *Korean J. Chem. Eng.* 2017, 34, 2099–2109, DOI: 10.1007/s11814-017-0102-5
- 44) Shieh, P.; Zhang, W.; Husted, K. E. L.; Kristufek, S. L.; Xiong, B.; Lundberg, D. J.; Lem, J.; Veysset, D.; Sun, Y.; Nelson, K. A.Cleavable Comonomers Enable Degradable, Recyclable Thermoset Plastics. *Nature* 2020, 583, 542–547, DOI: 10.1038/s41586-020-2495-2

- 45) Lloyd, E. M.; Cooper, J. C.; Shieh, P.; Ivanoff, D. G.; Nil, A.; Mejia, E. B.; Husted, K. E. L.; Costa, L. C.; Sottos, N. R.; Johnson, A.; Moore, J. S. Efficient Manufacture, Deconstruction, and Upcycling of High-Performance Thermosets and Composites. *ACS. Appl. Eng. Mater.* 2022, DOI: 10.1021/acsaenm.2c00115
- 46) Husted, K. E. L.; Shieh, P.; Lundberg, D. J.; Kristufek, S. L.; Johnson, J. A. Molecularly Designed Additives for Chemically Deconstructable Thermosets without Compromised Thermomechanical Properties. *ACS Macro Lett.* 2021, 10, 805–810, DOI: 10.1021/acsmacrolett.1c00255
- 47) Kantor, S. W.; Grubb, W. T.; Osthoff, R. C. The Mechanism of the Acid- and Base-Catalyzed Equilibration of Siloxanes. *J. Am. Chem. Soc.* 1954, 76, 5190–5197, DOI: 10.1021/ja01649a076
- 48) Osthoff, R. C.; Bueche, A. M.; Grubb, W. T. Chemical Stress-Relaxation of Polydimethylsiloxane Elastomers. *J. Am. Chem. Soc.* 1954, 76, 4659–4663, DOI: 10.1021/ja01647a052
- 49) Zheng, P.; McCarthy, T. J. A Surprise from 1954: Siloxane Equilibration Is a Simple, Robust, and Obvious Polymer Self-Healing Mechanism. *J. Am. Chem. Soc.* 2012, 134, 2024–2027, DOI: 10.1021/ja2113257
- 50) Debsharma, T.; Amfilochiou, V.; Alicja Wróblewska, A.; De Baere, I.; Van Paepegem, W.; Du Prez, F. E. Fast Dynamic Siloxane Exchange Mechanism for Reshapable Vitrimer Composites. *J. Am. Chem. Soc.* 2022, 144, 12280–12289, DOI: 10.1021/jacs.2c03518
- 51) Zhang, S.; Xu, X. Q.; Liao, S.; Pan, Q.; Ma, X.; Wang, Y. Controllable Degradation of Polyurethane Thermosets with Silaketal Linkages in Response to Weak Acid. *ACS Macro Lett.* 2022, 11, 868–874, DOI: 10.1021/acsmacrolett.2c00204
- 52) Ware, T.; Jennings, A. R.; Bassampour, Z. S.; Simon, D.; Son, D. Y.; Voit, W. Degradable, Silyl Ether Thiol-Ene Networks. *RSC Adv.* 2014, 4, 39991–40002, DOI: 10.1039/C4RA06997H
- 53) Shieh, P.; Nguyen, H. V. T.; Johnson, J. A. Tailored Silyl Ether Monomers Enable Backbone-Degradable Polynorbornene-Based Linear, Bottlebrush and Star Copolymers through ROMP. *Nat. Chem.* 2019, 11, 1124–1132, DOI: 10.1038/s41557-019-0352-4
- 54) Shieh, P.; Hill, M. R.; Zhang, W.; Kristufek, S. L.; Johnson, J. A. Clip Chemistry: Diverse (Bio)(Macro)Molecular and Material Function through Breaking Covalent Bonds. *Chem. Rev.* 2021, 121, 7059–7121, DOI: 10.1021/acs.chemrev.0c01282
- 55) Mark, J. E. Some Interesting Things about Polysiloxanes. *Acc. Chem. Res.* 2004, 37, 946–953, DOI: 10.1021/ar030279z
- 56) Johnson, A. M.; Husted, K. E. L.; Kilgallon, L. J.; Johnson, J. A. Orthogonally Deconstructable and Depolymerizable Polysilylethers via Entropy-Driven Ring-Opening Metathesis Polymerization. *Chem. Commun.* 2022, 58, 8496–8499, DOI: 10.1039/D2CC02718F

- 57) Bunton, C. M.; Bassampour, Z. M.; Boothby, J. M.; Smith, A. N.; Rose, J. V.; Nguyen, D. M.; Ware, T. H.; Csaky, K. G.; Lippert, A. R.; Tsarevsky, N. V.Degradable Silyl Ether–Containing Networks from Trifunctional Thiols and Acrylates. *Macromolecules* 2020, 53, 9890–9900, DOI: 10.1021/acs.macromol.0c01967
- 58) Bassampour, Z. S.; Budy, S. M.; Son, D. Y. Degradable Epoxy Resins Based on Bisphenol A Diglycidyl Ether and Silyl Ether Amine Curing Agents. *J. Appl. Polym. Sci.* 2017, 134, 44620, DOI: 10.1002/app.44620
- 59) Szychowski, J.; Mahdavi, A.; Hodas, J. J. L.; Bagert, J. D.; Ngo, J. T.; Landgraf, P.; Dieterich, D. C.; Schuman, E. M.; Tirrell, D. A. Cleavable Biotin Probes for Labeling of Biomolecules via Azide–Alkyne Cycloaddition. *J. Am. Chem. Soc.* 2010, 132, 18351–18360, DOI: 10.1021/ja1083909
- 60) Lemarié, F.; Beauchamp, E.; Legrand, P.; Rioux, V. Revisiting the Metabolism and Physiological Functions of Caprylic Acid (C8:0) with Special Focus on Ghrelin Octanoylation. *Biochimie* 2016, 120, 40–48, DOI: 10.1016/j.biochi.2015.08.002
- 61) Takeuchi, H.; Sekine, S.; Kojima, K.; Aoyama, T. The Application of Medium-Chain Fatty Acids: Edible Oil with a Suppressing Effect on Body Fat Accumulation. *Asia Pac. J. Clin. Nutr.* 2008, 17 Suppl 1, 320–323
- 62) Cypryk, M.; Apeloig, Y. Mechanism of the Acid-Catalyzed Si-O Bond Cleavage in Siloxanes and Siloxanols. A Theoretical Study. *Organometallics* 2002, 21, 2165–2175, DOI: 10.1021/om011055s
- 63) Lu, Y.-X.; Tournilhac, F.; Leibler, L.; Guan, Z. Making Insoluble Polymer Networks Malleable via Olefin Metathesis. *J. Am. Chem. Soc.* 2012, 134, 8424–8427, DOI: 10.1021/ja303356z
- 64) Zhang, V.; Kang, B.; Accardo, J. V.; Kalow, J. A. Structure-Reactivity-Property Relationships in Covalent Adaptable Networks. *J. Am. Chem. Soc.* 2022, 144, 22358–22377, DOI: 10.1021/jacs.2c08104
- 65) Della Martina, A.; Garamszegi, L.; Hilborn, J. G. Surface Functionalization of Cross-Linked Poly(Dicyclopentadiene). *React. Funct. Polym.* 2003, 57, 49–55, DOI: 10.1016/j.reactfunctpolym.2003.07.003
- 66) Defauchy, V.; Le Gac, P. Y.; Guinault, A.; Verdu, J.; Recher, G.; Drozdzak, R.; Richaud, E. Kinetic Analysis of Polydicyclopentadiene Oxidation. *Polym. Degrad. Stab.* 2017, 142, 169–177, DOI: 10.1016/j.polymdegradstab.2017.06.005